ANALYSIS FOR THERMAL BEHAVIOR AND ENERGY SAVINGS OF A SEMI-DETACHED HOUSE WITH DIFFERENT INSULATION STRATEGIES IN A HOT SEMI-ARID CLIMATE

Issam Sobhy[1,2], Abderrahim Brakez[1,2], Brahim Benhamou[1,2]

ABSTRACT

The purpose of this research is to assess thermal performance and energy saving of a residential building in the hot semi-arid climate of Marrakech (Morocco). The studied house is built as usual in Marrakech without any thermal insulation except for its external walls, facing East and West, which are double walls with a 5 cm air gap in between ("cavity wall" technique). The cavity wall effective thermal conductivity was carefully calculated taking into account both radiation and convection heat transfers. Experimental results, obtained from winter and summer monitoring of the house, show well dampening of air temperature, thanks to its thermal inertia. However, this temperature remained outside the standard thermal comfort zone leading to large cooling/heating load. Simulation results indicate that the cavity wall contributes to an overall reduction of 13% and 5% of the house heating and cooling loads respectively. Moreover, the addition of XPS roof thermal insulation significantly enhances the heating and cooling energy savings to 26% and 40% respectively.

KEYWORDS

dynamic simulation, monitoring, cooling & heating load, thermal insulation, cavity wall, energy saving

1. INTRODUCTION

In Mediterranean architecture, especially the vernacular Moroccan one, people created more easy-to-implement and climate-adapted architectural solutions to improve thermal comfort in buildings. However, the standardization of construction has not taken into account this ancestral bioclimatic architecture knowledge. This has resulted in blocks of buildings not adapted to the climate and requiring intensive active heating and cooling. Therefore, the building sector is currently one of the most energy-consuming sectors

1. Energy Processes Research Group, LMFE (URAC 27), Faculty of Science Semlalia, Cadi Ayyad University, Marrakech, Morocco
2. EnR2E laboratory, National Center of Studies and Research on Water and Energy CNEREE, Cadi Ayyad University, Marrakech, Morocco.
Corresponding author: BBenhamou@uca.ma

globally. This is particularly the case in Morocco with a share of 25% of the total energy consumption for the building sector [1]. This raises economic issues and negative environmental effects. Furthermore, it is often possible to fulfill thermal comfort requirements in modern buildings under low energy cost, taking advantage of the particular climate features by an appropriate design [2]. Significant reduction of the thermal load with improvements of winter and summer thermal comfort in buildings can be achieved by a better orientation, optimal windows size, thermal insulation, etc... [3,4]. It is well known that thermal insulation is one of the reliable passive systems that improve thermal comfort. Several researchers have studied its effect on buildings' thermal behavior through experiments and/or dynamic simulations [5-12]. Mohsen and Akash [6] studied the effect of thermal insulation of a typical residential building in Jordan. The comparison was made for three types of thermal insulation commonly used in Jordan (polystyrene, rock wool and air gap) during the cold period that lasts almost six months. By comparing three configurations of the building (i.e. without insulation, with wall insulation only and with walls and roof insulation), the authors found that the insulation of the walls with polystyrene leads to a reduction of the building's heating load by 36%, while wall insulation with an air gap reduces it by only 5.4%. The authors claim that the combination of polystyrene thermal insulation for the roof and the walls reduces the building's heating load by up to 78.6%. Nevertheless, the authors do not give any details regarding the building, the insulation thicknesses, the climate data and the simulation conditions. Guechchati et al. [7] conducted a dynamic simulation study of the effect of thermal insulation on energy consumption of a building located in Oujda (Morocco), which is in the Mediterranean moderately hot and cold climate zone. Simulations of several variants of the building led the authors to conclude that the insulation of the roof coupled with the external wall insulation both with 6 cm of polystyrene reduce the heating load by 16.4% and 19.8% respectively without and with double glazing. These values seem to be low considering the insulation thickness and that the climate is relatively cold. The authors do not give any validation of their TRNSYS model. Larsen et al. [8] studied the thermal behavior of two auditoriums in Argentina, the first located at the National University of La Pampa and the second at the University of General Pico. The former was constructed in a standard manner (referred to be the building's reference case) while the latter integrates thermal insulation of the envelope and natural ventilation. Air temperatures inside the two buildings were calculated by means of dynamic simulation. These calculations were validated through winter and summer monitoring with disparities beneath 1°C. Comparison of the simulation results for the two auditoriums led the authors to conclude that thermal insulation combined with shading devices and natural ventilation results in a 70% reduction of the cooling load. In winter, the authors found that the heating load has been decreased by 50% thanks to air heating through three solar air collectors.

Teoman Aksoy [9] studied numerically the relationship between the thickness of the thermal insulation material and the orientation of the walls of a test cell located in a cold region of Turkey (Elazig). The author used the finite difference method to solve the problem of transient heat transfer in the walls with and without thermal insulation. Energy saving in terms of heating load of the test cell may reach 19% to 78% for extruded polystyrene (XPS), depending on the insulation thickness. The optimal insulation thickness was found to be 10 cm. In contrast, Bolatturk [10] claims that the optimal insulation thickness using polystyrene in the warmest region of Turkey is 2 to 2.7 cm for the heating load and 3.2 to 3.8 cm for the cooling load depending on the city. These results were calculated using the degree-hours

method. Farhanieh and Sattari [11] conducted a numerical study on heat transfer through an external building wall with or without insulation in Teheran (Iran) which has a continental climate. An integrative model for predicting nonlinear behavior of the wall with the nodal network approach is used. The authors show that 2.5 cm standard insulation material leads to a significant reduction of the heat flux up to 67% in winter, which corresponds to a 45% heating energy saving. Byrne et al. [12] investigated experimentally the thermal behavior of a two storey old home located in a temperate oceanic maritime climate zone of Ireland. The home was retrofitted with pumped polystyrene bead insulation in the 10 cm external wall cavity. The ceiling was also thermally insulated. The authors compared field data, including walls and roof surfaces temperature and heat fluxes, before and after the fixing of the cavity wall and ceiling insulation. The authors concluded that predicted values of heat losses using standard material properties did not reflect the actual values achieved in situ. Indeed, the calculated thermal resistances based on standard materials properties, overestimated the reduction in heat losses by nearly 50% and 20% respectively through the ceiling and the walls. In addition, the authors found that 10 cm of polystyrene thermal insulation led to heat loss reduction of 56% and 35% through the walls and the roof respectively.

Thermal insulation is one of the key elements of the Moroccan Thermal Regulation for Construction [13] which has been effective since November 2015. Sick et al. [14] presented the background of this project. The authors conducted dynamic simulations of seven building types and analyzed the effect of the buildings' envelope parameters on the heating/cooling loads in five climate zones of Morocco. Conditioned and unconditioned buildings were simulated using TRNSYS software. The authors deduced the heating/cooling energy demand as well as free-floating temperature statistics. The heating/cooling energy demands are calculated based on the set points of 20°C for heating and 24°C for cooling. Several variants of the buildings were considered including a reference case (no insulation) and cases with insulation for both walls, roof and floor. Moreover, two buildings' orientations are simulated. Thermal insulation thickness was varied from 2 to 8 cm, 4 to 8 cm and 2 to 6 cm respectively for the walls, the roof and the floor with a thermal conductivity of 0.04 $W.m^{-1}.K^{-1}$. The window-to-wall ratio was varied from 15 to 45% with windows' U-value changing from 3.3 to 1.3 $W.m^{-2}.K^{-1}$ and windows' g-value ranging from 75% to 62%. For each type of the buildings, an occupation scenario was scheduled along with fixed air change of 30 $m^3.h^{-1}$ per person. External shading was considered in summer (May 15 to September 15) during the day. The results are presented for collective residential buildings and public administration buildings. For Marrakech, the authors found that the mean total thermal load of the collective residential building is reduced to 75 $kWh.m^{-2}$/year. This reduction was obtained with 15% of the window-to-wall ratio, double glazing (U-value = 2.6 $W.m^{-2}.K^{-1}$ and g-value = 70%) and thermal insulation of 6, 8 and 4 cm respectively for the walls, the roof and the floor. The resulting building's thermal load is substantially consisting of cooling demand. Its value is still high as noted by the authors. Although the calculated thermal load is a mean value over the five floors of the building, it is believed that the floor's thermal insulation contributes significantly to the high thermal load value found in Marrakech compared to the other climate zones where the heating need is much higher. Indeed, the same behavior was obtained by the authors for the city of Fes, with a climate that leads to considerable heating and cooling demand. The case of Ifrane (considerable heating and no cooling demand) is remarkable as thermal insulation of the floor is mandatory due to the high heating demand. Thermal insulation of the

collective residential building leads to low values of heating/cooling energy demand of almost 50 kWh.m^{-2}/year. The effect of the building's floor thermal insulation was investigated by Sobhy et al. [15] in the case of two floors single house located in Marrakech. These authors showed that this thermal insulation is not required as the heating demand is low. Moreover, this thermal insulation increases the cooling demand as it prevents the house benefiting from the soil thermal inertia. For this reason, thermal insulation of the house floor in contact with the soil is not considered in the present study.

The "cavity wall" consists of two walls separated by an air space and anchored together with metal ties for strength. This system is widely used as a low cost thermal insulation technique in many parts of the world [16-18]. The main function of such wall construction is to increase thermal resistance while preventing water infiltration. Several design guides are available in the literature providing predictive data of the thermal resistance of the cavity wall [17]. However, the R-value coefficients provided in these guides are essentially limited to radiation as heat transfer mode inside the air space. While heat conduction may be neglected, thanks to the low thermal conductivity of air, convection may play a major role especially for large width cavities. Furthermore, radiation heat flux may be reduced inside the cavity wall by means of a radiant barrier. Aviram et al. [16] carried out an experimental investigation to estimate convection heat transfer flux inside a 1.2 x 1.2 m² cavity wall with different widths. The authors found that Nusselt number ranged from 12 to 2.0 for 7.8 cm and 4.0 cm width cavities respectively. Thus, the air cavity offers more thermal resistance at low width. The authors also conducted a numerical study which results indicate that the flow regime changed from turbulent at 8.0 cm to laminar at 4.0 cm of cavity width. Moreover, the authors found that the flow regime becomes purely conductive at a cavity width of 2.5 cm. Al-Sanea et al. [18] investigated numerically a west-facing cavity wall, partly filled with an insulation material, under steady periodic conditions using the climate data of Riyadh (Saudi Arabia). The authors studied many configurations to determine the optimum insulation technique. Different widths of the air space in the cavity wall have been considered. The effective thermal resistance of the air space, calculated at the mean temperature of 32 °C, ranges from 0.70 m².K.W^{-1} to 0.15 m².K.W^{-1} respectively with and without a radiant barrier for a width of 4 cm. These are values based on the ASHRAE guidelines [19] which completely ignore convection heat transfer inside the cavity wall.

Thermal insulation is obviously one of the key elements for the reduction of the heating load in buildings. However, high thermal insulation may lead to summer overheating, especially in hot climates. Thus, the cooling load has to take into account the heating needs reduction as well. For hot semi-arid climates, like the one in Marrakech (Morocco), the buildings' cooling load is the most significant compared to the heating one, as the former is present during more than six months while the later lasts four months at the most. The present research aims at studying the effect of thermal insulation on thermal performance and energy savings of a two-floor semi-detached house in the hot semi-arid climate of Marrakech. The objective here is to conduct theoretical and experimental analysis in order to determine the effect of the roof and walls thermal insulation on the heating and cooling loads of the studied house. For thermal insulation of the walls, the "cavity wall" technique is used. As mentioned above, coarse estimation of the cavity wall thermal resistance may be found in the literature. In this paper, a careful calculation of this thermal resistance is conducted, by considering both radiation and convection heat transfers.

2. BUILDING DESCRIPTION

The studied building, called Nassim, is a modern-type and semi-detached house according to the national classification [1]. It is built as usual in Marrakech without any thermal insulation except for its walls which are of "cavity wall" type with a 5 cm air gap [16-18]. The house has a floor area of 70 m^2, with two façades, oriented east and west, giving onto small gardens. The house consists of two floors and a terrace with a laundry room. The architectural plans are given in Annex 1. The main entrance is located in the western façade. Thermo-physical properties of the house construction materials are indicated in Table 1. These properties were obtained from the library of the BINAYATE software, dedicated to the RTCM conformity control of the buildings' envelope in Morocco [20].

TABLE 1. Thermo-physical properties of construction materials [20].

Material	Thermal capacity ($kJ.kg^{-1}.K^{-1}$)	Thermal conductivity ($W.m^{-1}.K^{-1}$)	Density ($kg.m^{-3}$)
Cement mortar	1.000	1.800	2500
Air gap without radiant barrier (cavity wall)	1.007	0.324*	1.20
Air gap with radiant barrier (HCS technique)	1.007	0.120*	1.20
Concrete block	0.830	0.559	768
Red clay brick	0.741	0.190	918
Plaster	1.000	0.569	1150
Concrete slab	1.000	2.500	2500
Concrete	1.000	2.300	2350
Ceramic tiles	0.840	1.300	2300
Extruded polystyrene (XPS)	1.45	0.032	32.5

**Calculations' details are given in Annex 2.*

North and south external walls of the Nassim house are adjoined to the neighboring houses of the same type. The overall thickness of these walls (including the neighboring ones) is 44 cm with four layers (2 cm of cement mortar, two concrete blocks of 20 cm each and 2 cm of cement mortar); this leads to an overall U-value of 1.10 $W.m^{-2}.K^{-1}$. The roof is composed of five layers (1 cm of plaster, 16 cm hollow bricks with steel beams, 4 cm of reinforced concrete, 10 cm of cement mortar and 2 cm of ceramic tiles) with an overall U-value of 2.24 $W.m^{-2}.K^{-1}$. The first floor slab is composed of five layers (1 cm of plaster, 16 cm of hollow bricks with steel beams, 4 cm of reinforced concrete, 7 cm of cement mortar and 1 cm ceramic tiles) with an overall U-value of 2.44 $W.m^{-2}.K^{-1}$. The low-level floor is a slab-on-grade made up of five layers (50 cm of pebbles, 7 cm of reinforced concrete, 7 cm of cement mortar and 1 cm of ceramic tiles); this leads to an overall U-value of 1.86 $W.m^{-2}.K^{-1}$. The façade walls have a thickness of 28 cm, made up of five layers (1.5 cm of cement mortar, 10 cm red clay brick, air gap of 5 cm, 10 cm red clay brick and 1.5 cm of cement mortar). In order to calculate the overall heat transmission coefficient of these walls, it is necessary to correctly estimate

the air gap thermal resistance. To this end, a careful calculation of the effective thermal conductivity of the air gap, is conducted taking into account both convection and radiation heat transfers. The details of these calculations are presented in Annex 2. It can be seen that convection heat flux accounts for 35% of the total heat transfer between the internal surfaces of the cavity wall. Neglecting convection heat flux, which is the prevalent case in the literature as mentioned above [17-19], leads to an error of 30% in the estimation of the air gap thermal resistance. The effective thermal conductivity of the 5 cm air gap in the cavity wall is given in Table 1. The resulting overall thermal transmittance (U-value) of the façade walls is 0.72 $W.m^{-2}.K^{-1}$.

The Nassim house windows are French ones with wooden frame and single glazing. Some windows are equipped with shading devices. The doors are either metallic or wooden ones. The details of the windows and doors constitution are given in Table 2. Table 3 presents the window-to-wall ratio (WWR) for each façade wall and each floor. The glazing area in the eastern façade is much higher than the one in the western façade especially in the ground floor. The total WWR for the East and West oriented façades of the studied house are 16% and 10% respectively, leading to a total WWR of 13% for the house.

TABLE 2. Constitution of windows and doors (the zones are defined in Annex 1, Fig. 1.2).

House zones	Z1	Z2	Z3	Z4	Z5	Z6	Z7	Z8
Windows type	3	4	2	3	-	-	4	2
Doors type	1	5	1	-	1	1	-	6

Type 1: metallic frame with 6 mm translucent glazing (U-value = 5.68 $W.m^{-1}.K^{-1}$; g-value = 0.482) [21]
Type 2: wooden frame with 4 mm single glazing without any shading (U-value = 5.8 $W.m^{-1}.K^{-1}$; g-value = 0.862) [21]
Type 3: 4 mm single glazing with internal wooden flaps
Type 4: 4 mm single glazing with external fixed shading device (*Moucharaby*)
Type 5: 6 cm wooden door (main entrance)
Type 6: metallic door

TABLE 3. Window-to-wall ratio.

Walls orientation	Ground floor		1st floor		Terrace	
	West	East	West	East	West	East
Window-to-wall ratio (%)	11.3%	22%	11.3%	15.1%	3.9%	3.9%

3. WEATHER CONDITIONS

The house under study is located in Marrakech, Morocco (Latitude 31°38'N, Longitude 8°03'W, Altitude 426 m), and 200 km away from the Atlantic coast and 80 km from the Atlas mountains. The climate of Marrakech is classified as a hot semi-arid one with very hot summers and relatively cold winters as well as large differences between day and night

air temperatures that may reach 20°C. A weather station was installed on the terrace of the Nassim house. It measures: air temperature, relative air humidity, global solar radiation, wind velocity and direction. Table 4 shows some measured meteorological data. The on-site measured meteorological data are used to perform the validation of our computer code.

TABLE 4. Some on-site measured meteorological data (BS200 Campbell weather station).

Year	Months	Max. Temperature (°C)	Min. Temperature (°C)	Average Temperature (°C)	Average Humidity (%)	Global solar irradiation, on horizontal plane (kW/m²)
2013	July	45.9	17.5	29.9	36.1	211
	August	45.1	17.4	30.9	35.6	205
	September	37.5	16.4	24.0	60.7	156
	October	34.2	11.6	22.2	59.9	147
	November	31.3	7.0	17.5	57.1	117
	December	23.7	3.4	13.5	60.0	101
2014	January	26.7	4.6	12.6	66.5	100
	February	25.3	6.7	13.7	66.9	128
	March	31.9	7.1	16.5	58.2	165
	April	35.4	9.6	21.3	50.7	207
	May	41.6	13.0	24.2	45.0	222
	June	40.7	14.6	24.7	47.2	231
	July	43.0	16.5	27.0	46.2	247

4. NUMERICAL SIMULATION

The thermal behavior of the house was simulated through transient multi-zone modeling by means of TRNSYS software [21], with a time step of 1 hour. TRNSYS is a one of the complete and extensible (modular) simulation environments for the transient simulation of thermal systems, including buildings. The multi-zone building model incorporated in TRNSYS is constantly being updated and it is still one of the most accurate and comprehensive simulation tools worldwide in this respect. It consists in dividing the house into several thermal zones where air temperatures are calculated through thermal balances [22]. The thermal balance of a thermal zone, represented by an air node including the thermal capacity of the zone volume, is given by [22],

$$\dot{Q}_{\iota} = \dot{Q}_{surf,i} + \dot{Q}_{inf,i} + \dot{Q}_{vent,i} + \dot{Q}_{g,c,i} + \dot{Q}_{cplg,i} + \dot{Q}_{solar,i} + \dot{Q}_{ISHCCI,i} \quad (1)$$

Where,

$\dot{Q}_{surf,i}$ is the convection heat flux from the zone opaque surfaces given by,

$$\dot{Q}_{surf,i} = U_{w,i}\, A_{w,i}(T_w - T_{air}) \quad (2)$$

$\dot{Q}_{inf,i}$ is the heat flux associated to the air infiltration (air flow from outside only) given by,

$$\dot{Q}_{inf,i} = \dot{V}\, \rho\, C_p(T_{ext,i} - T_{air}) \quad (3)$$

$\dot{Q}_{vent,i}$ is the heat flux associated to air ventilation (air flow from a user-defined source) given by,

$$\dot{Q}_{vent,i} = \dot{V}\ \rho\ C_p(T_{vent,i} - T_{air}) \quad (4)$$

$\dot{Q}_{g,c,i}$ is the internal convection heat flux due to occupation and equipment.

$\dot{Q}_{cplg,i}$ is the convection heat flux due to airflow from/to the neighbor air nodes given by,

$$\dot{Q}_{cplg,i} = \dot{V}\ \rho\ C_p(T_{zone,i} - T_{air}) \quad (5)$$

$\dot{Q}_{solar,i}$ represents the fraction of solar radiation entering an air node through external windows which is immediately transferred to the internal air.

$\dot{Q}_{ISHCCI,i}$ is the absorbed solar radiation by the internal shading devices of the zone and directly transferred to the internal air.

The air temperature in a given thermal zone is deduced from the energy balance below [22],

$$C_i \frac{d}{dt} T_i = \dot{Q}_i \quad (6)$$

The thermal load is deduced from the energy balance of the thermal zone heated and cooled to the set temperatures to be fixed,

$$C_i \frac{d}{dt} T_i = \dot{Q}_i - P_i \quad (7)$$

Where, P_i is the power output for the considered thermal zone. P_i is negative for heating and positive for cooling. The value of P_i is calculated by assuming that the air thermal zone temperature change, when power is supplied, is linear [22].

Figure 1 presents the assembly panel window of our TRNSYS project, including all the involved modules (Types) and links.

FIGURE 1. Assembly panel window.

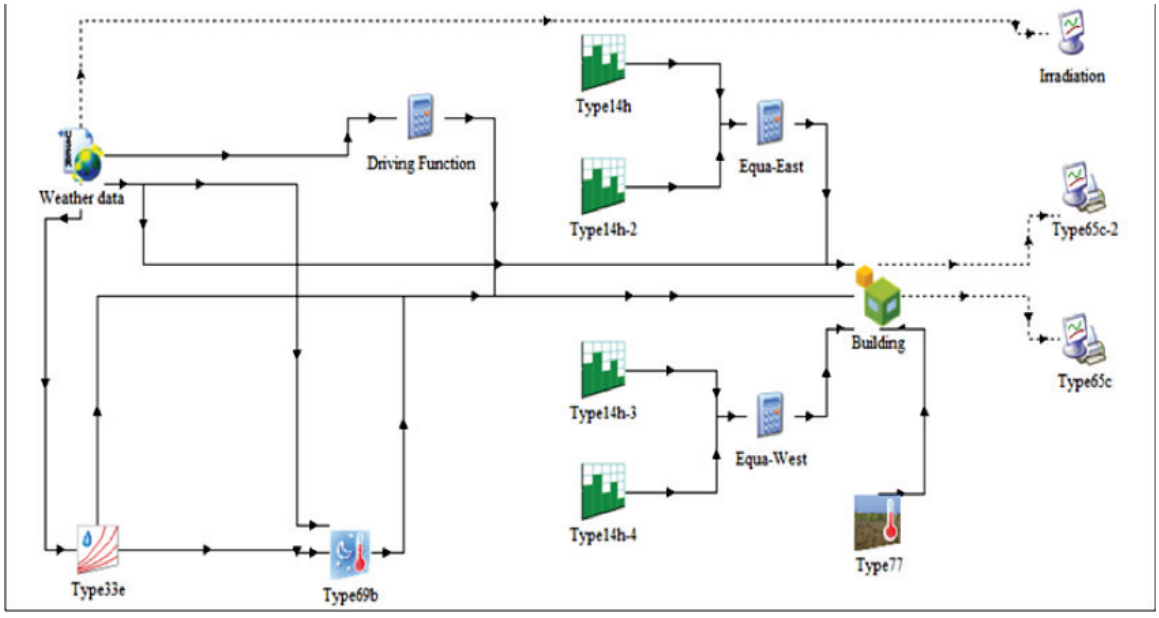

The house is divided into eight zones: three on the ground floor (Z1-Z3), four zones on the first floor (Z4-Z7) and a single zone (Z8) for the laundry (refer to the architectural plans in Annex 1). The heating and cooling loads in each zone are calculated on the basis of

the set air temperatures of 20°C and 26°C, respectively according to the Moroccan standard NM ISO 7730 [23]. This standard sets the humidity comfort at 60% and 55% respectively in summer and winter.

Simulations were performed using the following assumptions:

- Initial air temperature and humidity are taken equal to 20°C and 50% respectively in all zones.
- No internal heat generation (unoccupied house).
- The doors and windows are closed all the time (no free cooling).
- The window shutters opening is scheduled depending on the season (see section 8).
- Constant infiltration rate of 0.5 ACH is assumed for all zones.
- The absorption coefficients of the ceramic tiles in the terrace and exterior painting are set to 0.8 and 0.75 respectively.
- The walls external emissivity is taken equal to 0.9.
- Convection heat transfer coefficients at the outside surfaces hout are calculated using (Eq. 8) which takes into account the wind velocity V [24],

$$h_{out} = 2.8 + 3.2 * V \quad (8)$$

- TYPE 77 of TRNSYS was used to calculate the ground temperature, considering that the mean soil surface temperature is equal to the mean annual air temperature of Marrakech which is here 20°C [25, 26].

In order to take into account thermal bridges, the reinforced concrete skeleton system of the house is considered in the TRNSYS simulation. The reinforced concrete posts and beams are defined in the TRNSYS3D plug-in as independent surfaces as it can be seen in Figure 2, where thermal bridges are delimited by the horizontal (concrete beams) and vertical (concrete posts) lines. Thermal conductivity of reinforced concrete is attributed to these surfaces in TRNBuild type, leading to an overall heat transmission coefficient of 3.7 $W.m^{-2}.K^{-1}$ for thermal bridges.

For the sake of thermal conditioning of the soil and the building in relation with the local meteorological data, the simulation covers two consecutive years. The results presented hereafter concern the second year.

FIGURE 2. 3D model implemented in Google SketchUp with thermal bridges for TRNSYS : (a) West view, (b) East view.

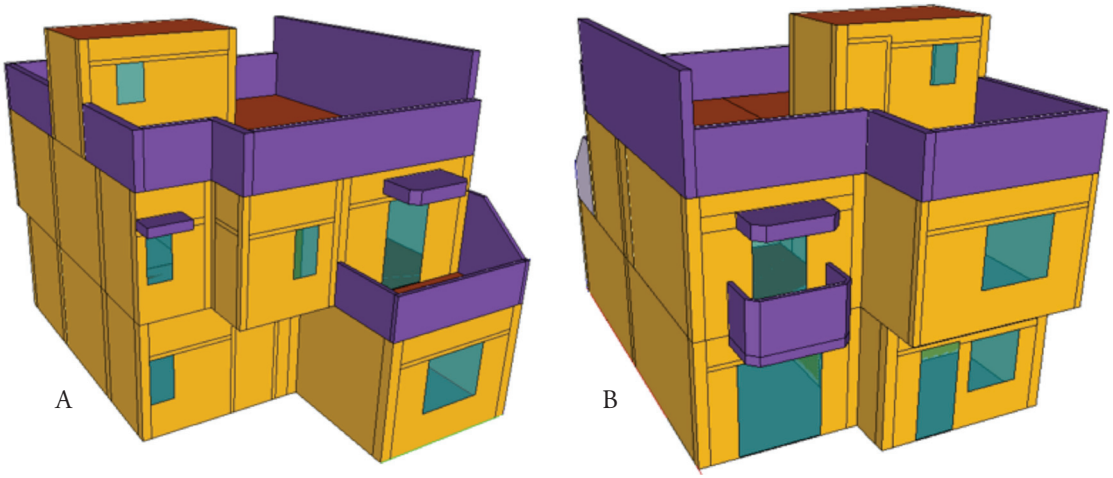

5. MONITORING OF THE HOUSE

The Nassim house was monitored during 10 days of the heating season (from December 27th, 2013 to January 5th, 2014) and two months of the cooling season (July and August 2013) by measuring air temperature and relative humidity in each of the eight zones considered in the simulation. Data loggers TESTO174H, that measure air temperature and relative humidity with errors of 0.5°C and 3%, respectively, are installed in each zone. These data acquisition systems are hanged from the ceiling at 1.5m above the floor in the middle of each zone. Air temperature and relative humidity are recorded every 12 minutes. The building was unoccupied so that the doors and the windows were closed during the monitoring period. The main objective of this monitoring is to validate our computer code, as well as to analyze the real thermal behavior of the house.

6. MONITORING RESULTS

6.1. Measured temperature profile in winter

Figures 3.a and 3.b show the evolution of the daily average air temperature measured in each zone of the house. These air temperatures vary between 14.5°C and 16.7°C for the ground floor zones (Fig. 3.a), while for the first floor these air temperatures variation range between 12.9°C and 16.4°C (Fig. 3.b). In addition, the average outdoor air temperature varies between 10.4°C and 14.8°C. Thus, air temperatures of all zones remained below the heating set point of 20°C. Nevertheless, the variations of the daily average air temperature during the monitoring period inside each zone do not exceed 1.8°C on the ground floor, 2.6°C on the first floor and 3°C in zone Z8 (Laundry) while this variation is 4.4°C outside the house. It is clear from Figure 3.a that the studied house has a modest thermal inertia. Indeed, the phase shift between the occurrence of air temperature minima on the ground floor and outside is around three days. The same phase shift was found on the first floor (Fig. 3.b). Furthermore, we notice that zone Z4 is hotter than zone Z5 although they have the same glazed area, the same volume, and are located on the same east side of the first floor. Air temperature difference between these two zones is attributed to the shading of the 2 m height adjoining wall on the roof of Z5. Moreover, part of the Z4 external wall is oriented south and thus receives more solar gains than Z5. Furthermore, Z7 is hotter than Z5 and Z6, because it is heated by the laundry room (Z8). The latter is the hottest zone in the house with large air temperature variations between day and night. Indeed, this zone is characterized by a low volume and contains a black metal door facing east. Also, the laundry room is characterized by three façades with two single glazing windows without shutters, facing east and west, and a thin roof concrete slab of 12 cm. The daily average air temperature in this zone varies between 14.7°C and 17.6°C.

Figure 4 shows the evolution of the hourly average measured air temperature for each floor; the outside air temperature is also reported. The outside air temperature has a minimum value of 3.4°C (recorded on 31/12/2013 at 7:00 AM) and a maximum value of 21.4°C (which occurs on 03/01/2014 at 3:00 PM). There is significant amplitude of the outside air temperature oscillations. Indeed, this amplitude (half the peak-to-peak air temperature difference during the same day) during the monitoring period may reach up to 8.3°C in a day. Inside the house, the daily air temperature amplitude varies between 0.2°C to 0.3°C for the ground floor, 0.2°C to 0.5°C for the first floor, and 1°C to 2°C for the laundry room. This clearly shows that the house's thermal inertia dampens the outside air temperature oscillations.

FIGURE 3A. Daily average measured air temperatures on the ground floor zones in winter.

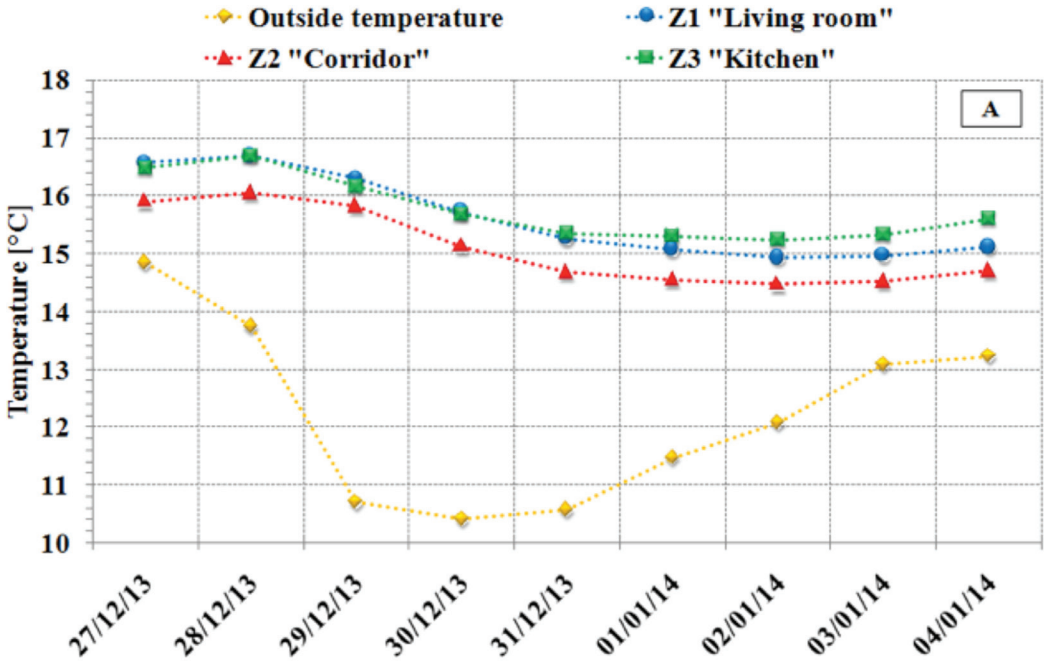

FIGURE 3B. Daily average measured air temperatures on the first floor zones and laundry in winter.

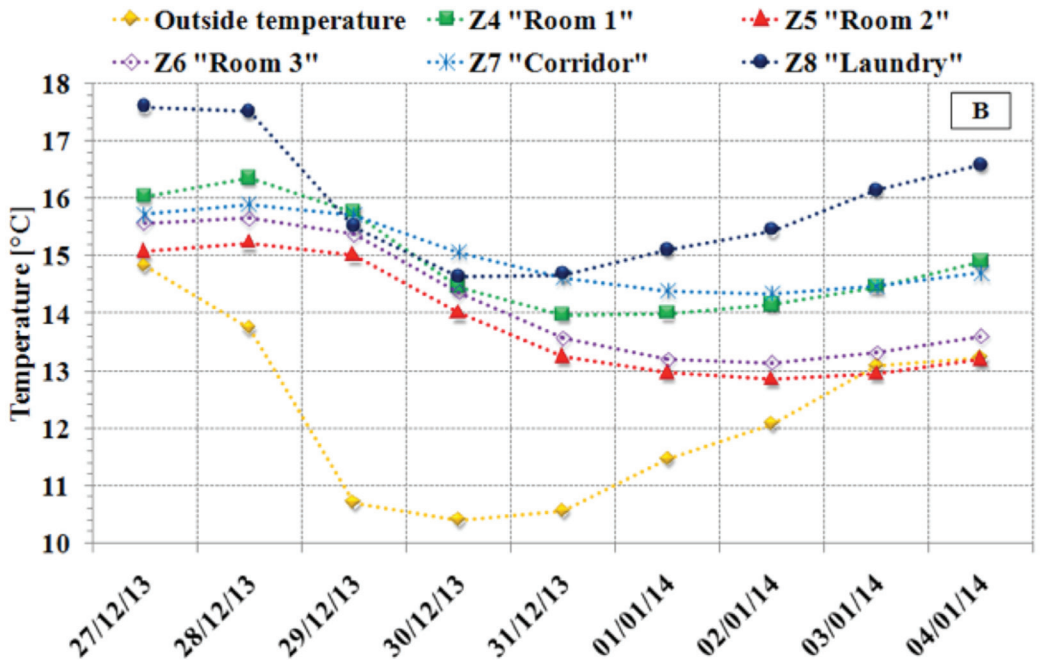

However, as mentioned above, the laundry room (Z8) has weak thermal inertia that explains the relative wide oscillations of its temperature. Furthermore, the ground floor air temperature is always higher than that of the first floor with a difference of 0.4°C to 1.7°C. This is quite normal due to the heat losses through the roof on the first floor. The average air temperature

for each floor during the monitoring period was 15.5°C, 14.5°C and 15.9°C respectively on the ground floor, the first floor and the laundry room. Thus, air temperature in the house remains far from the thermal comfort zone leading to a large heating load.

Figures 5.a and 5.b show the time evolution of the measured air humidity inside and outside the house. The outdoor air humidity varies between 18% and 97%. Inside the house,

FIGURE 4. Hourly average measured air temperatures in winter.

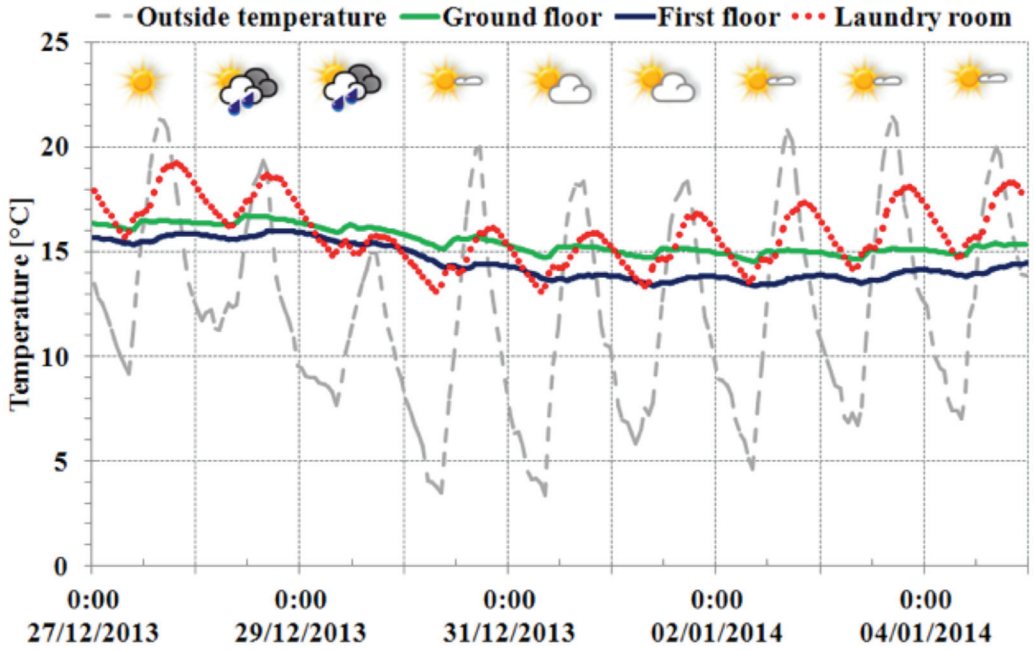

FIGURE 5A. Hourly average measured air humidity on the ground floor zones in winter.

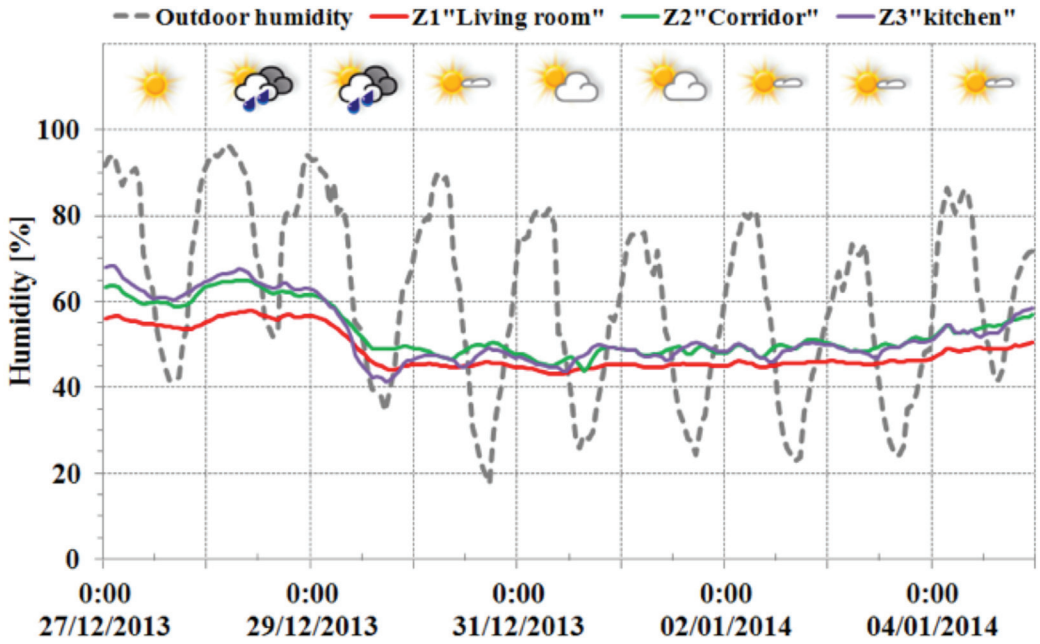

FIGURE 5B. Hourly average measured air humidity on the first floor zones and laundry in winter.

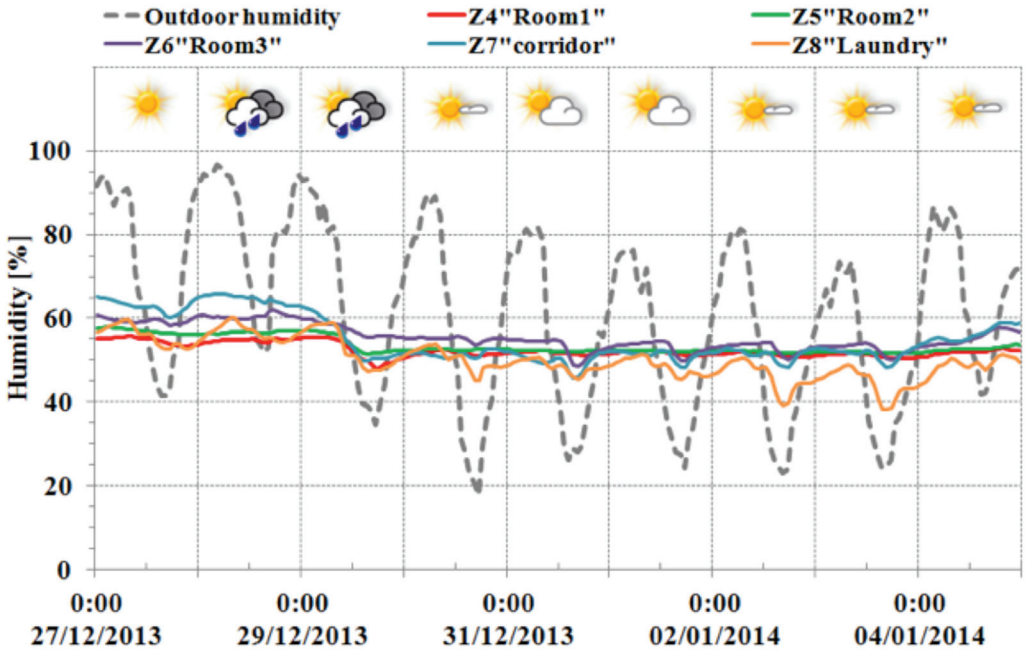

air humidity varies between 41% and 68% on the ground floor, while on the first floor it ranges between 46% and 66%. In the laundry room, the air humidity ranges between 38% and 60%. Therefore, during the monitoring period, it is noted that the air humidity in the house remains in the range of the standard thermal comfort zone [27].

6.2. Measured temperature profile in summer

As mentioned above, the summer monitoring period lasts for 62 days. For clarity reasons, the results are presented here for the hottest week (25 to 31 July, 2013). Figures 6.a and 6.b show the evolution of the daily average air temperature measured in each zone of the house during the selected week of the monitoring period; the outside air temperature is also reported. The daily average air temperature varies between 29.5°C and 31.8°C on the ground floor zones (Fig. 6.a), while on the first floor its variations range between 31.8°C and 34.6°C (Fig. 6.b). Thus, air temperature in all zones remained above the commonly adopted set point of 26°C for residential buildings cooling. In addition, it is clear from Figs. 6.a and 6.b that variations of the daily average air temperature inside each zone do not exceed 1.4°C on the ground floor, 2°C on the first floor, 5.2°C in the laundry room, while these variations reach 9.4°C outside the house. These variations are of the same order of magnitude as during the winter monitoring for the ground and first floor, although the outside daily average air temperature variations are more than twice as much as during the winter monitoring. Zones Z5 and Z6 have the same daily average air temperature (Fig. 6.b). Indeed, these two zones, located on the first floor, have the same glazed area and the same volume, although they do not have the same orientation. Similar behavior has been identified during the winter monitoring (Fig. 3.b). Furthermore, Z7 is the coldest zone on the first floor, as its roof is not exposed to solar radiation. Indeed, the laundry room (Z8) almost covers the entire corridor (Z7) ceiling. The zone Z8 has the same behavior as depicted in the winter monitoring as it is the hottest zone in the house with large air temperature variations between day and night.

FIGURE 6A. Daily average measured air temperatures on the ground floor zones in summer.

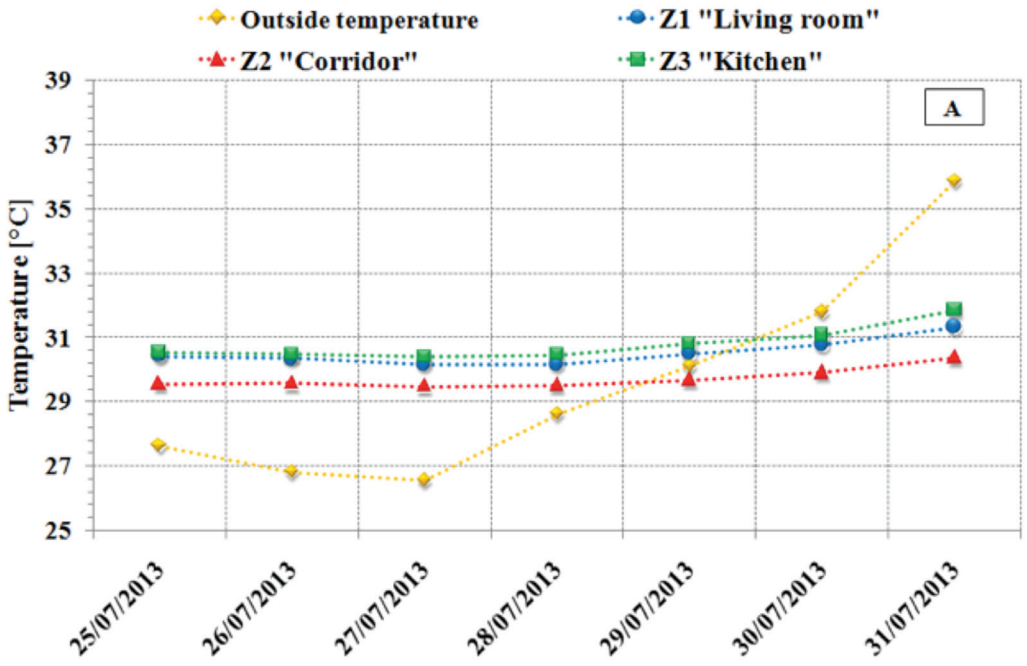

FIGURE 6B. Daily average measured air temperatures on the first floor zones and laundry in summer.

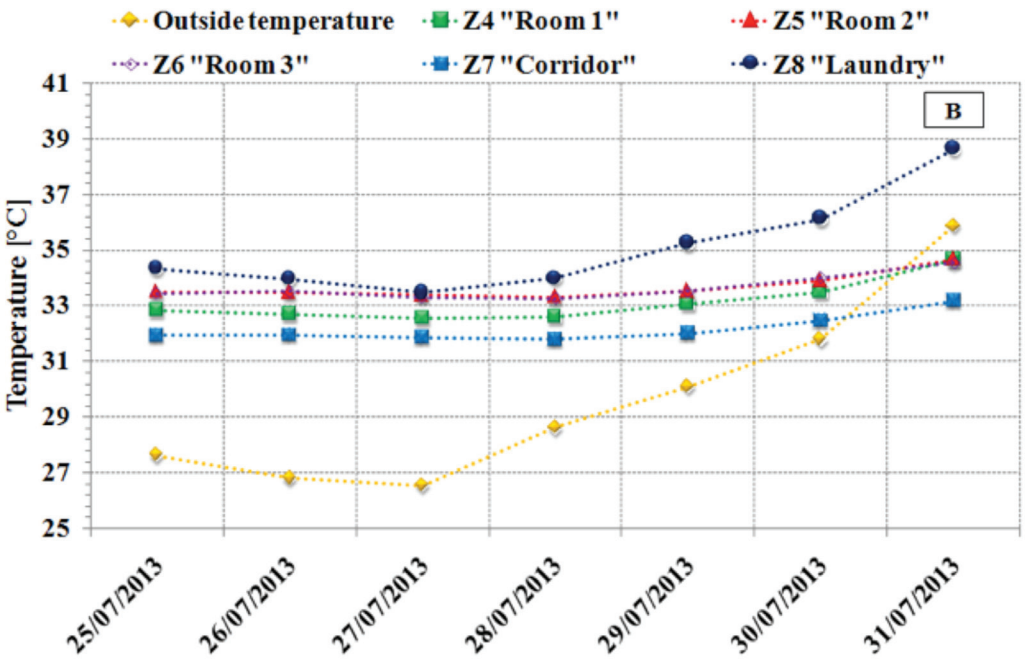

FIGURE 7. Hourly average measured air temperatures in summer.

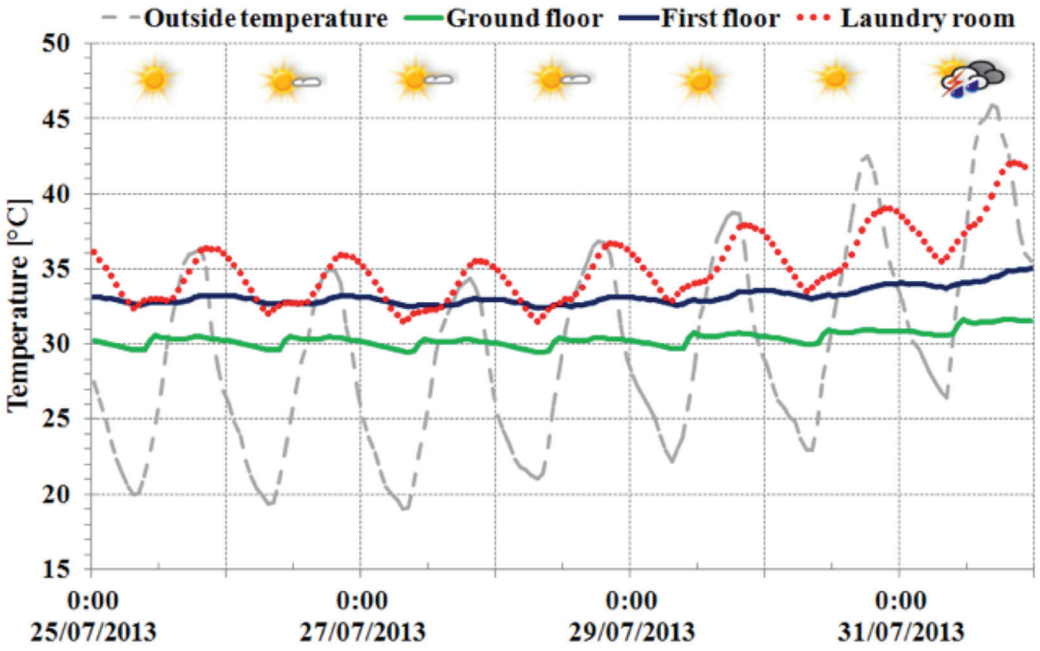

Figure 7 shows the hourly average measured air temperature evolution on each floor. The outside air temperature evolves between 19°C and 45.9°C. There is a significant daily amplitude of this temperature, which may goe up to 9.7°C. Inside the house, this amplitude varies between 0.4°C to 0.5°C on the ground floor, 0.3°C to 0.6°C on the first floor and 1.8°C to 3.3°C in the laundry room. These amplitudes are of the same order of magnitude as in winter. This leads to the conclusion that the studied house effectively dampens the outside air temperature oscillations thanks to its thermal inertia. Furthermore, the first floor air temperature is always higher than that of the ground floor with a difference of 2.1°C to 3.5°C, due to the solar gains through the roof. The average air temperature on each floor during the selected week was 30.3°C, 33.1°C and 35.1°C respectively on the ground floor, the first floor and the laundry room. Thus, air temperature in the house remains outside the human thermal comfort zone leading to a large cooling load.

Figures 8.a and 8.b show time variations of air humidity inside and outside the house. The outdoor air humidity exhibits variations between 6% and 86%, while inside the house, these variations are in between 29% and 45% on the ground floor, 22% and 38% on the first floor and 13% and 37% in the laundry room. Therefore, air humidity inside the house remains between 30% and 50% which a good level for thermal comfort [27]

7. COMPARISON OF THE SIMULATION AND EXPERIMENTAL RESULTS

In order to assess the validity of our computer code, a comparison between simulation and monitoring results was performed both in winter and summer. Figures 9.a and 9.b present an example of the calculated and measured air temperatures in winter and summer for the first floor zone Z4. The calculated and measured air temperatures maximum deviation is 0.8°C in winter (Fig. 9.a) and 0.6°C in summer (Fig. 9.b). In the other zones of the house, calculated and measured air temperatures have the same behavior with deviations of the same order of

FIGURE 8A. Hourly average measured air humidity on the ground floor zones in summer.

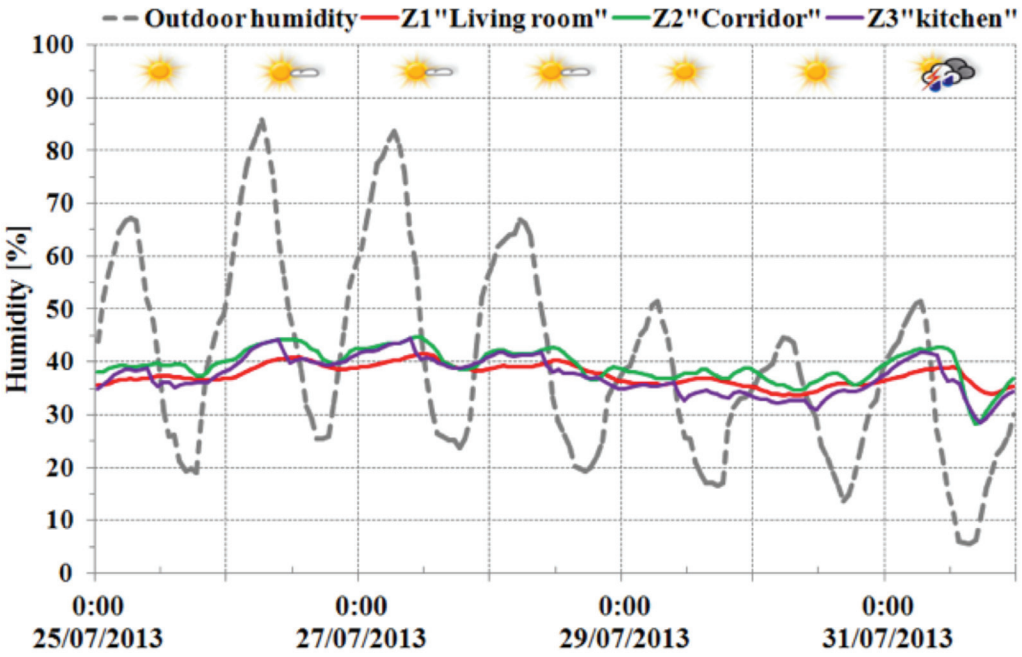

FIGURE 8B. Hourly average measured air humidity on the first floor zones and laundry in summer.

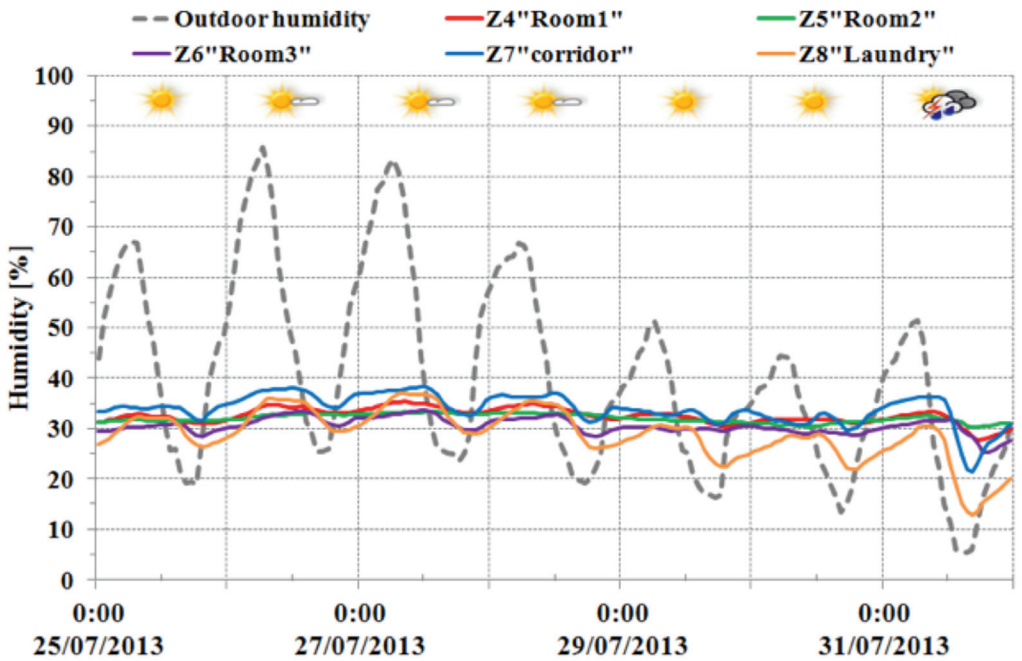

magnitude as the one in Z4. Table 5 shows the maximum absolute differences between the measured and calculated air temperatures for all zones of the house. The distributions of these air temperature differences are also reported. It is clear that these differences do not exceed 1°C; essentially in winter this difference is always less than 0.8°C except for zones Z1 and Z3, where it may reach 0.9°C, while in summer it is less than 0.8°C for all zones except for zone

Z3. Careful examination of Table 5 shows that the zone where the air temperature is the most consistent is Z4 in summer and Z7 in winter. The Z4 zone has an absolute deviation of less than 0.6°C, in addition 99% of the differences are less than or equal to 0.5°C. By contrast, in winter zone Z7 has an absolute difference of 0.6°C, and 96% of the differences are in the

FIGURE 9A. Hourly average measured and calculated air temperatures in winter, in Z4.

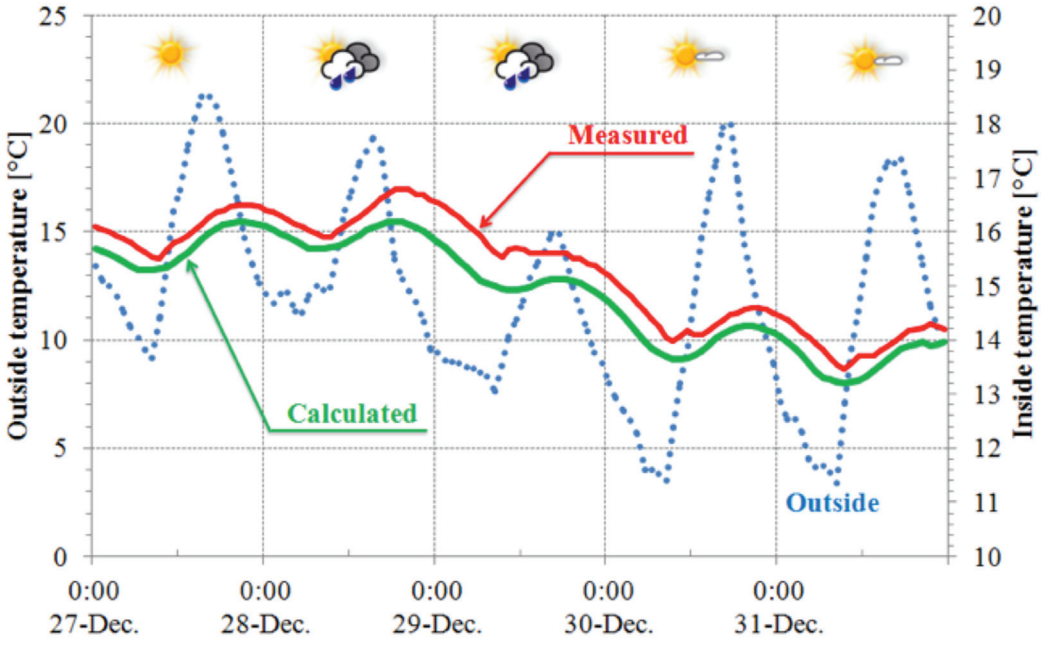

FIGURE 9B. Hourly average measured and calculated air temperatures in summer, in Z4.

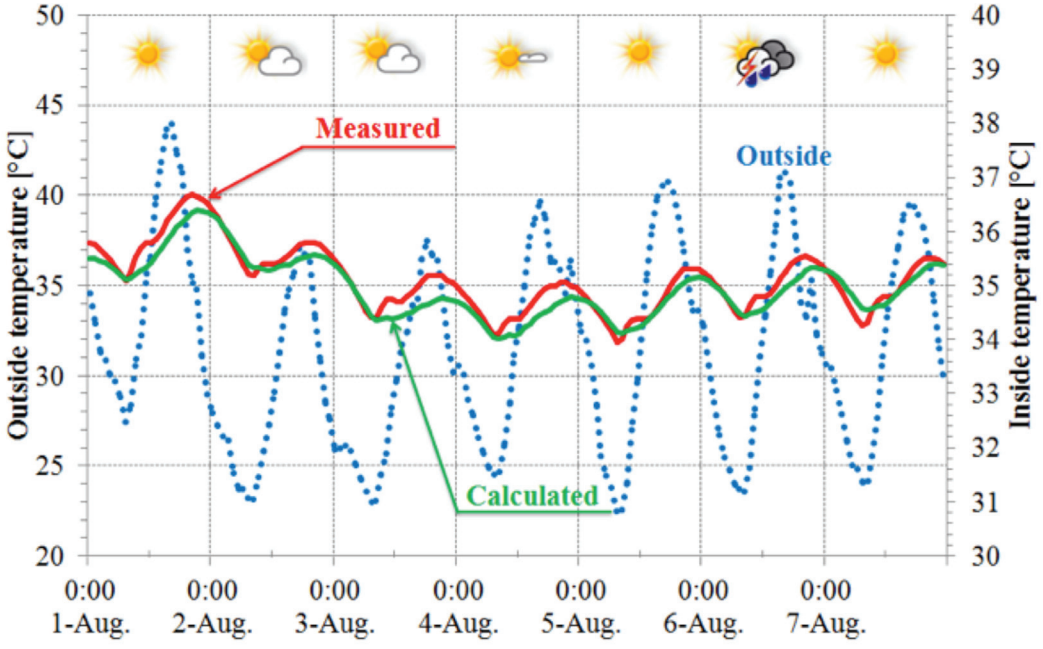

range of 0 to 0.5°C. It can be deduced from Table 5 that more than 99% of the differences between the measured air temperatures and the calculated ones all over the house are lower than 1°C. Therefore, it can be concluded that there is a very good agreement between our experimental and numerical results.

TABLE 5. Maximum absolute deviations and distribution of air temperature differences between simulation results and the measurements.

		Z1	Z2	Z3	Z4	Z5	Z6	Z7
Maximum deviation	Summer	0.7	0.5	1.2	0.6	0.8	0.6	0.8
	Winter	0.9	0.6	0.9	0.8	0.7	0.7	0.6
Differences between 0°C and 0.5°C	Summer	95%	97%	71%	99%	90%	93%	70%
	Winter	64%	92%	78%	75%	93%	93%	96%
Differences between 0.5°C and 1°C	Summer	5%	3%	22%	1%	10%	7%	30%
	Winter	36%	8%	22%	25%	7%	7%	4%
Differences between 1°C and 1.5°C	Summer	0%	0%	7%	0%	0%	0%	0%
	Winter	0%	0%	0%	0%	0%	0%	0%

8. SIMULATION RESULTS

In this section the validated computer code is used for the calculation of the heating and cooling loads of the studied house. Furthermore, different insulation strategies are considered for the reduction of these thermal loads. Calculations were conducted using standard meteorological data of Marrakech, which represents a typical meteorological year for the period 2000-2009 [28]. As mentioned above, all the windows and doors are closed all the time (unoccupied house). However, in order to calculate the thermal load of the house, it is essential to take into account direct solar gains. To this end, a scheduling of the opening of the shading devices is introduced. During cold months (from November 1st to March 31th), the movable flaps are opened from 8:00AM to 11:00AM for east orientation and from 3:00PM to 6:00PM for west orientation. During hot months (from April 1st to October 31th) all the moving shading devices are opened during the night from 8:00PM to 6:00AM.

8.1. Heating and cooling loads of the house

Figures 10.a and 10.b show the annual calculated heating and cooling loads of different zones of the house. From Fig. 10.a, it is clear that heating is needed for all zones, as predicted by the monitoring results. The heating load is present starting from November to March. Zones Z2 and Z7 (corridors in the ground and first floors) exhibit the lowest heating load on the ground and first floors respectively. Indeed, these zones have one external wall facing west with small glazing areas veiled by wood fixed shutters (Moucharaby). The other zones exhibit almost the same heating needs as they all have similar glazing areas. Zones Z5 and Z6 have a slightly high heating load, because of the 2 m high neighboring south wall shading on their roof. This was pointed out during the winter monitoring (section 6.1).

Figure 10.b presents the annual cooling loads of different zones in the house. As for the heating load, the zone Z2 exhibits the lowest cooling load. Moreover, this zone has almost

the same heating and cooling needs. Zone Z2 is indeed located on the ground floor and then benefits from the soil thermal inertia as well as zones Z1 and Z3. However, as mentioned above and contrary to Z1 and Z3, the zone Z2 has a small single glazing window facing west and veiled by wood fixed shutters. The first floor zones Z4, Z5 and Z6 have almost the same

FIGURE 10A. Annual heating loads of the house [kWh/m²].

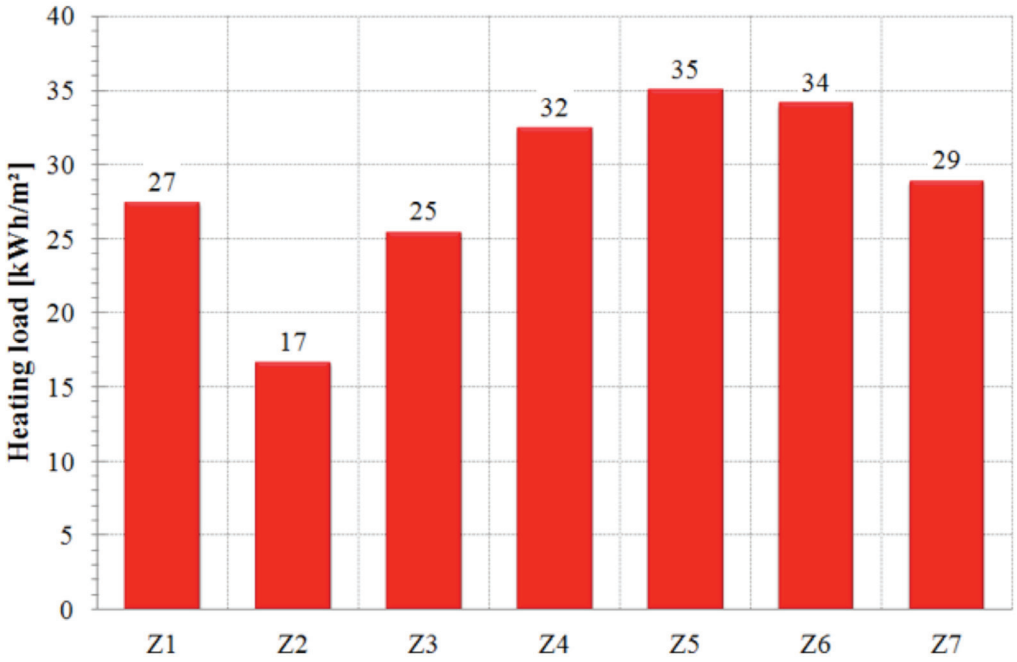

FIGURE 10B. Annual cooling loads of the house [kWh/m²].

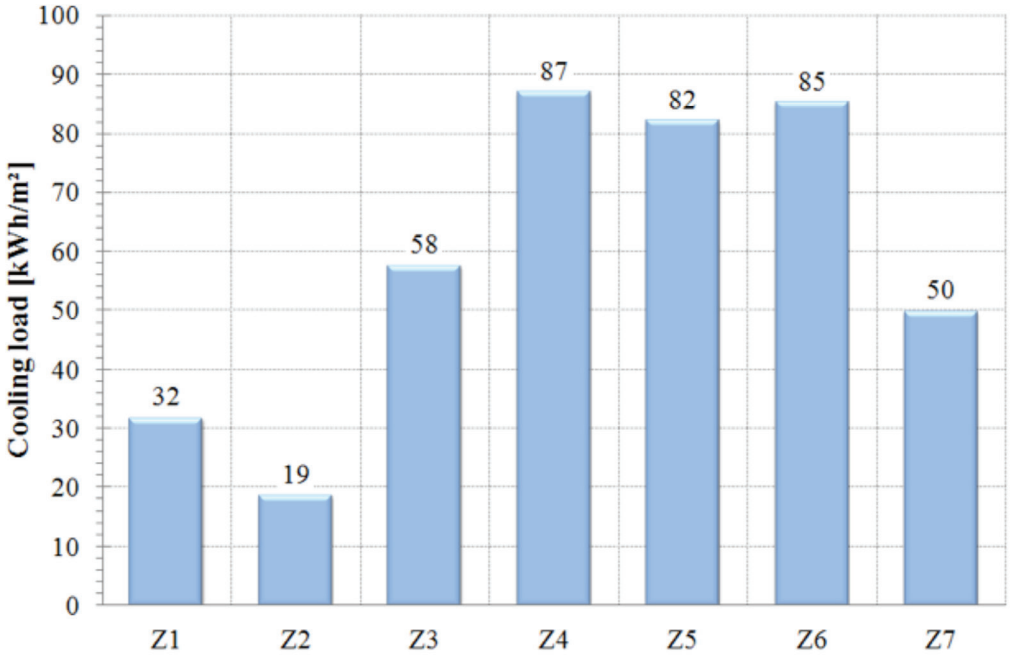

cooling load. Indeed, the roofs of these zones are similarly exposed to solar radiations. By contrast, as the ceiling of the zone Z7 is almost covered by the laundry room (Z8), its cooling needs are the lowest on the first floor. From these results we notice that the cooling load of the house is more than twice larger than its heating load.

8.2. Effect of thermal insulation

To assess the thermal performance of the studied building, as a typical semi-detached house in Marrakech, and evaluate the energy savings that may result from its retrofit, a parametric study is conducted with different envelope thermal insulation strategies. Six configurations of the house are considered and listed in Table 6. The first one is the real house, while the others correspond to the lack of wall insulation through the air gap (reference case) or the introduction of the roof thermal insulation. Two roofs' thermal insulation strategies are considered: the first one uses 4 cm of XPS and the second concerns a double slab with a 5 cm air gap and a radiant barrier commonly called hollow core slab (HCS). Comparison of the heating and cooling loads of these configurations will allow for the determination of the effect of each thermal insulation strategy.

TABLE 6. Studied configurations of the building.

	Walls thermal insulation with 5 cm air gap	Roof thermal insulation with 4 cm XPS	Hollow Core Slab with 5 cm air gap
#1 (Real house)	**YES**	NO	NO
#2 (Reference case)	NO	NO	NO
#3	NO	**YES**	NO
#4	**YES**	**YES**	NO
#5	NO	NO	**YES**
#6	**YES**	NO	**YES**

Figure 11 presents the annual heating and cooling loads of the house for each configuration. Configurations #1 (real house) and #2 (reference case), show that the 5 cm air gap wall insulation slightly reduces the heating and cooling loads of the house by 13% and 5% respectively. Comparison of configurations #1 and #4 reveals that the XPS roof insulation clearly diminished the heating and cooling loads by 15% and 37% respectively. Moreover, compared to the reference case (#2), the heating loads of configuration #3 and #4 are reduced by 10% and 26% respectively while their cooling loads drop down by 30% and 40% respectively. It can be concluded that thermal insulation of the walls has more significant effect than the roof insulation in winter, but in summer the roof insulation is more significant than the walls' insulation. The combination of these insulations (configuration #4) reveals a beneficial interaction, as the resulting energy savings of 26% and 40%, respectively in terms of heating and cooling needs are greater than the addition of the energy savings obtained separately.

Alternatively, to the XPS for the roof insulation, a double slab with a 5 cm air gap is considered. This technique, called hollow core slab (HCS), was used by many researchers [29, 30]. The internal surfaces of the slabs are equipped with radiant barriers (such as aluminum foil or plastic film) which stop long wave radiation heat transfer through the air gap. This HCS technique leads to an equivalent air gap thermal conductivity of 0.12 $W.m^{-2}.K^{-1}$. The details of this calculation are given in Annex 2. To study the effect of the HCS technique, two configurations of the house are simulated (Table 6). The first one corresponds to the reference

FIGURE 11. Annual heating/cooling loads of different configurations of the house [kWh/m²].

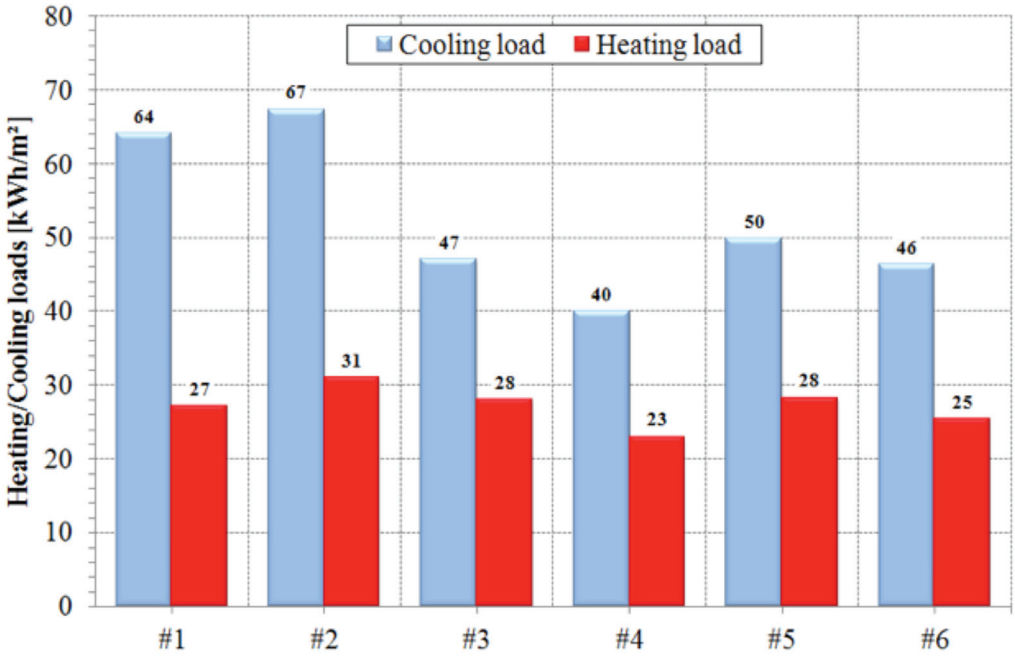

case with the HCS (configuration #5) and the second one is the real house with the HCS (configuration #6). Comparison of configurations #5 and # 2 (reference case) shows that the HCS is able to reduce the heating and cooling loads by 10% and 25% respectively. The combination of the walls and roof insulation using air gaps (configuration #6) leads to the house thermal load reduction by 19% and 31% for heating and cooling respectively compared to the reference case.

It follows from the previous results that thermal insulation of the roof using XPS leads to better results than the HCS technique. Indeed, the heating and cooling loads with XPS thermal insulation are lower by around 9% and 15% respectively, compared to the HCS technique. It is interesting to mention that thermal performance of the latter may be enhanced by ventilation during hot periods to cool the lower slab and then the ceiling [31, 32]. Furthermore, our results do not exhibit any overheating in summer due to thermal insulation, even though the house windows were continuously closed (no free cooling). This is due to the fact that the walls were insulated by a 5 cm air gap whose equivalent thermal conductivity is ten times that of standard insulation materials. Indeed, it was checked that wall insulation with such standard insulation materials leads to overheating and increases the house's annual cooling load by at least 20% [33].

Finally, it is interesting to mention that the Moroccan Thermal Regulation for Construction - RTCM - imposes a maximum of 61 kWh/m²/year for the thermal load of residential buildings in the Marrakech climate zone [13]. From Fig. 11, it is clear that only the real house with 4 cm XPS roof thermal insulation (configuration #4) satisfies this requirement with a very slight deflection.

9. CONCLUSION

A numerical and experimental study of a modern-type and semi-detached house in Marrakech (Morocco) was performed. The house is built as usual in Marrakech without any thermal

insulation except for its walls which are of "cavity wall" type with a 5 cm air gap. The experimental study was carried out through the house monitoring during summer 2013 and winter 2013-2014 by means of air temperature and humidity measurements in different rooms of the house. The experimental results have shown that the air temperature for the two floors of the house was almost constant during the monitoring periods, leading up to the conclusion that the studied house dampens well the outside air temperature oscillations thanks to its thermal inertia. However, the air temperature in the house remains outside the standard thermal comfort zone causing large cooling and heating loads, although air humidity inside the house was fairly comfortable.

The numerical study was conducted using the multi-zone thermal model of TRNSYS software. Good agreement was found between numerical and experimental results with a maximum absolute deviation not exceeding 0.9°C in winter and 1.2°C in summer. The effect of thermal insulation of the building's envelope on its cooling/heating loads is assessed through the comparison of six configurations of the house. The results show that the 4 cm XPS roof insulation reduces the heating and cooling loads by 10% and 30% respectively, compared to the reference case (no envelope insulation). Furthermore, the 5 cm air gap cavity walls contribute to an overall energy savings of 13% and 5% in terms of heating and cooling loads respectively, compared to the un-insulated house. The combination of these insulations leads to 26% and 40% of energy saving for the heating and cooling needs respectively, revealing beneficial interaction in summer. In addition, the use of the hollow core slab (HCS) technique with 5 cm air gap and a radiant barrier reduces the heating and cooling loads by 19% and 31% respectively compared to the reference case (no envelope thermal insulation).

Our results do not exhibit any summer overheating due to thermal insulation, even though the house's windows were continuously closed (no free cooling). In contrast, it was checked, in another work, that the walls' insulation with standard material, such as XPS, causes summer overheating leading to an increase of the house annual cooling load by at least 20%.

Finally, it is important to mention that thermal inertia is a significant parameter as it has major incidence on the house thermal performance. This parameter is worthy of more attention.

ACKNOWLEDGMENT

This study is a part of the RafriBat project financially supported by the PARS grant from the Hassan II Academy of Sciences and Techniques, Morocco.

NOMENCLATURE

A_w	Area of the wall (m^2)
C_p	Specific heat of the air ($kJ.kg^{-1}.K^{-1}$)
g-value	Fraction of solar radiation transmitted by the glazing of a window (%)
h_{out}	Convection heat transfer coefficient at exterior surface of the walls ($W.m^{-2}.K^{-1}$)
h_m	Convection heat transfer coefficient inside the cavity wall ($W.m^{-2}.K^{-1}$)
H	Height of the cavity wall (m)
k_{eff}	Effective thermal conductivity of the air space in the cavity wall ($W.m^{-2}.K^{-1}$)
k_{air}	Thermal conductivity of air ($W.m^{-2}.K^{-1}$)
L	Air space width in the cavity wall (m)
Nu	Nusselt number

R Effective thermal resistance of the air space in the cavity wall, R-value ($m^2.K.W^{-1}$)
Ra_L Rayleigh number
T_1 Internal surface temperature of the outside wall in the cavity wall system (K)
T_2 Internal surface temperature of the inside wall in the cavity wall system (K)
T_{ext} Ambient air temperature (K)
T_{air} Air temperature inside the thermal zone (K)
T_{vent} Temperature of the ventilation air (K)
T_w Air temperature of the wall's inside surface (K)
U Overall heat transmission coefficient, U-value ($W.m^{-2}.K^{-1}$)
V Wind velocity ($m.s^{-1}$)
$\dot{V}$ Mass flow rate of infiltration or ventilation air ($kg.s^{-1}$)

Indices

conv Convection heat flux
rad Thermal radiation flux
cond Conduction heat flux
g Global heat flux

Greek symbols

υ Kinematic viscosity ($m^2.s^{-1}$)
α Thermal diffusivity ($m^2.s^{-1}$)
β Expansion coefficient
g Gravitational acceleration ($m.s^{-2}$)
σ Stefan-Boltzmann constant ($W.m^{-2}.K^{-4}$)
ε Surface emissivity
ρ Density of the air (kg/m^3)
ϕ Heat flux between the internal surfaces of the cavity wall ($W.m^{-2}$)

Abbreviations

XPS Extruded polystyrene
HCS Hollow core slab
RTCM Moroccan Thermal Regulation for Construction
WWR Ratio of the windows area to the total considered wall

REFERENCES

[1] Moroccan Agency for Energy Efficiency, AMEE, Morocco. www.aderee.ma (Accessed on June 30, 2016).
[2] Givoni B. Man, Climate and Architecture. 2nd Edition. Harvard University Press, Cambridge, MA,U.S.A, 1976.
[3] Jaber S, Ajib S. Optimum technical and energy efficiency design of residential building in Mediterranean region. Energy and Buildings 2011; 43: 1829-1834.
[4] Santamouris M, Kolokotsa D. Passive cooling dissipation techniques for buildings and other structures: The state of the art. Energy and Buildings 2013; 57: 74–94.
[5] Al-Homoud MS. Performance characteristics and practical applications of common building thermal insulation materials. Building and Environment 2005; 40: 353-366.
[6] Mohsen MS, Akash BA. Some Prospect of Energy Saving in Building. Energy Conversion Management 2001; 42: 1307-1315.
[7] Guechchati R, Moussaoui MA, Mezrhab Ahm, Mezrhab Abd. Simulation de l'effet de l'isolation thermique des bâtiments : Cas du centre psychopédagogique SAFAA à Oujda. Revue des Energies Renouvelables 2010; 13: 223-232.

[8] Larsen SF, Filippín C, Beascochea A, Lesino G. An experience on integrating monitoring and simulation tools in the design of energy-saving buildings. Energy and Buildings 2008; 40: 987-997.
[9] Teoman Aksoy U. A numerical analysis for energy savings of different oriented and insulated walls in the cold climate of Turkey – Simulation-based study. Energy and Buildings 2012; 50: 243-250.
[10] Bolatturk A. Optimum insulation thicknesses for building walls with respect to cooling and heating degree-hours in the warmest zone of Turkey. Building and Environment 2008; 43: 1055-1064.
[11] Farhanieh F, Sattari S. Simulation of energy saving in Iranian buildings using integrative modelling for insulation. Renewable Energy 2006; 31: 417-425.
[12] Byrne A, Byrne G, Davies A, Robinson AJ. Transient and quasi-steady thermal behaviour of a building envelope due to retrofitted cavity wall and ceiling insulation. Energy and Buildings 2013; 61: 356-365.
[13] RTCM (2015), Moroccan Thermal Regulation in Construction. Available at (Accessed on June 30, 2016) http://www.aderee.ma/index.php/fr/publicationsetmedias/publications
[14] Sick F, Schade S, Mourtada A, Uh D, Grausam M. Dynamic building simulations for the establishment of a Moroccan thermal regulation for buildings. Journal of Green Building, 2014; Vol. 9; Issue 1.
[15] Sobhy I, Brakez A, Benhamou B. Effect of thermal insulation and ground coupling on thermal load of a modern house in Marrakech. International Renewable and Sustainable Energy Conference (IRSEC). DOI: 10.1109/IRSEC.2014.7059797, pp. 425-430. Ouarzazate (Morocco), 17-19 October 2014.
[16] Aviram DP, Fried AN, Roberts JJ. Thermal properties of a variable cavity wall. Building and Environment 2001; 36: 1057-1072.
[17] CIBSE guide, Section A3, Thermal Properties of Building Structures.
[18] Al-Sanea SA, Zedan MF, Al-Ajlan SA, Abdul Hadi AS. Heat transfer characteristics and optimum insulation thickness for cavity walls. J Thermal Env Bldg Sci 2003; 26: 285–307.
[19] ASHRAE, (1997), chap. 24: "thermal and water vapor transmission data" in Handbook of Fundamentals, American Society of Heating, Refrigerating and Air-Conditioning Engineers, Inc., Atlanta.
[20] BINAYATE Software, Assessment of the buildings' energy performance and control of the conformity with the Moroccan Thermal Regulation in the Construction. Available via: www.aderee.ma/index.php/fr/publicationsetmedias/publications (Accessed on June 30, 2016).
[21] Klein SA. A Transient System Simulation Program. Solar Energy Laboratory, University of Wisconsin-Madison, WI, USA, 2000.
[22] TRNSYS17. Reference manual, volume 5. Multizone Building modeling, Madison, WI, USA, 2010.
[23] NM ISO 7730 (2010), Institut Marocain de Normalisation, Ergonomie des ambiances thermiques-Détermination analytique et interprétation du confort thermique par le calcul des indices PMV et PPD et par des critères de confort thermique local.
[24] Incropera FP, DeWitt DP. Fundamentals of Heat and Mass Transfer. John-Wiley and Sons, 1985.
[25] Kusuda T, Achenbach PR. Earth Temperature and Thermal Diffusivity at Selected Stations in the United States. ASHRAE Transactions, 1965, Vol. 71, Part 1.
[26] Celini CF. Modélisation et positionnement de solutions bioclimatiques dans le batiment résidentiel existant. Doctorate Thesis, L'université Lyon 1 Claude Bernard, France, June 2008.
[27] ASHRAE, chap. 8: "thermal comfort" in Handbook of Fundamentals, American Society of Heating, Refrigerating and Air-Conditioning Engineers Inc., Atlanta, 1997.
[28] METEONORM, 2014, V7.0.22.8. Available via www.meteonorm.com.
[29] Chang PC, Chiang CM, Lai CM. Development and preliminary evaluation of double roof prototypes incorporating RBS (radiant barrier system). Energy and Buildings 2008; 40: 140–147.
[30] Tong S, Li H, Zingre KT, Wan MP, Victor WC, Wong SK, Thian Toh WB, Leng Lee IY. Thermal performance of concrete-based roofs in tropical climate. Energy and Buildings 2014; 76: 392–401.
[31] Biwole PH, Woloszyn M, Pompeo C. Heat transfers in a double-skin roof ventilated by natural convection in summer time. Energy and Buildings 2008; 40: 1487-1497.
[32] Dimoudi A, Androutsopoulos A, Lykoudis S. Summer performance of a ventilated roof component. Energy and Buildings 2006; 38: 610-617.
[33] Sobhy I, Brakez A, Benhamou B. Impact of the RTCM technical requirements on a residential building located in Marrakech, Proceedings of the 4th International Thermal Conference AMT'2016, Meknes (Morocco) 19-20 March 2016 (in French).
[34] Mills A. F. Basic Heat and Mass Transfer. second edition, University of California at Los Angeles, ISBN 0-13-096247-3, 1999.

[35] Hollands K. G. T., Unny TE, Raithby GD, Konicek L. Free convective heat transfer across inclined air layers. J. Heat Transfer 1976; 98: 189-193.
[36] El Sherbiny S. M., Raithby G. D., Hollands K. G. T. Heat transfer by natural convection across vertical and inclined air layers. J. Heat Transfer 1982; 104: 96-102.

ANNEX 1

FIGURE 1.1. Photos of the Nassim house, West view (a) and East view (b)

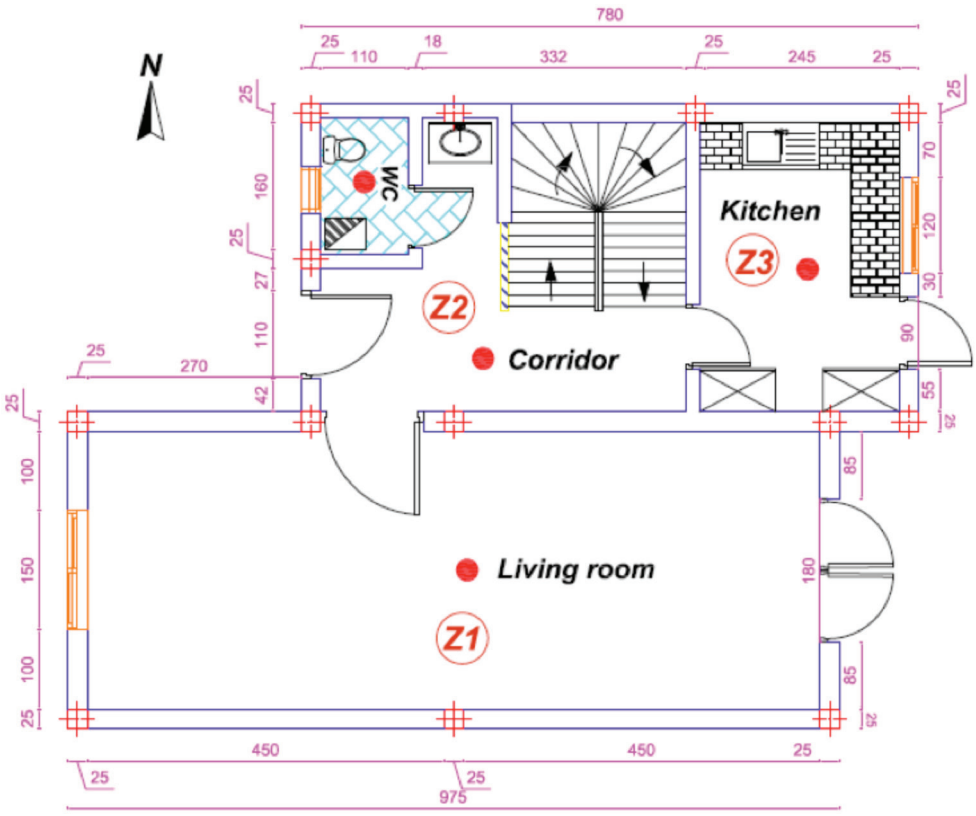

(A) Ground Floor

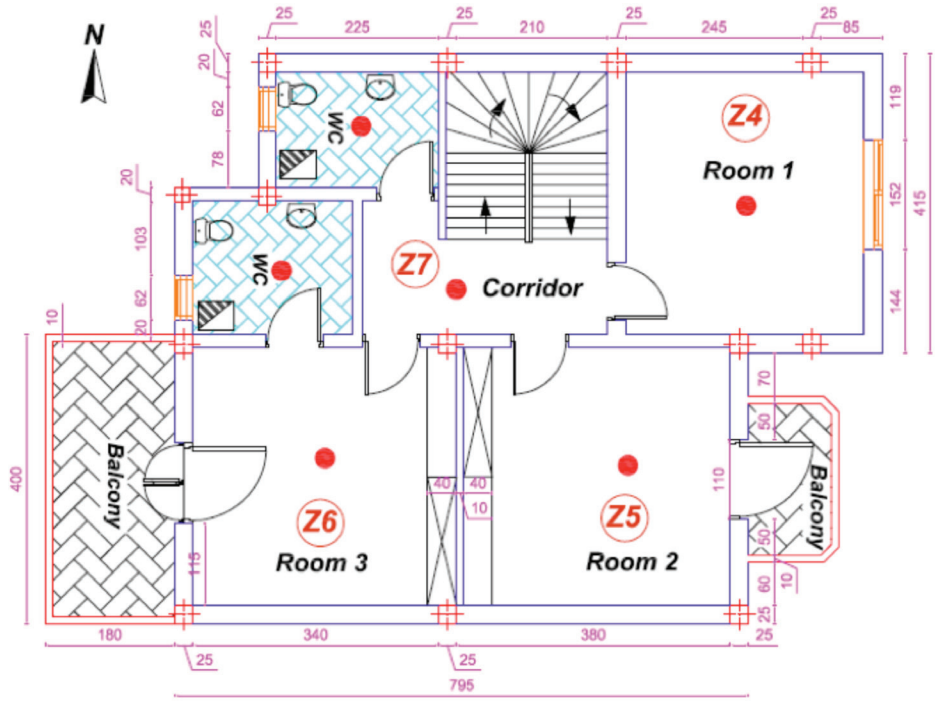

(B) First Floor

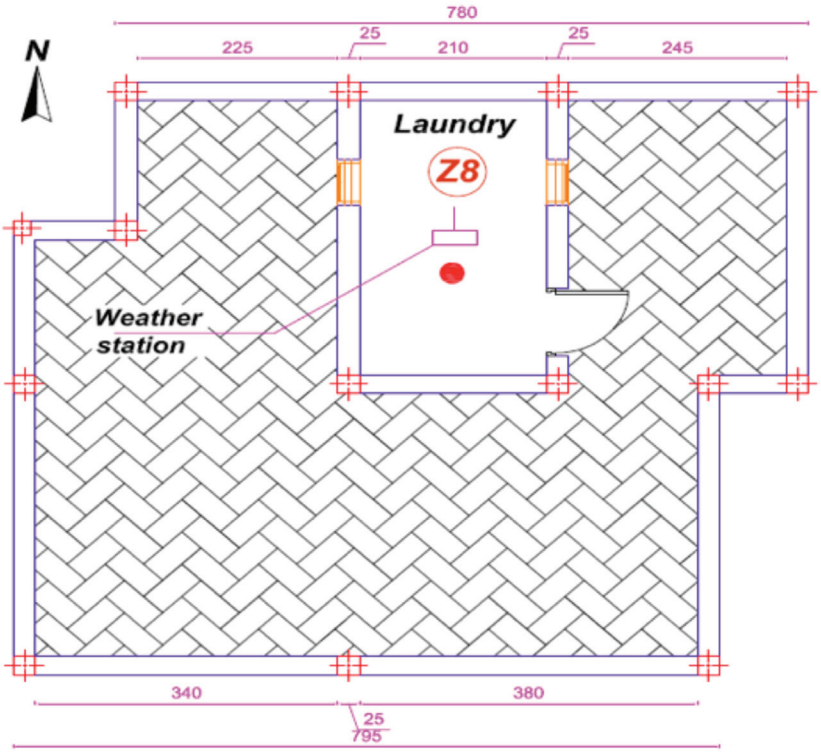

(C) Terrace

Fig. 1.2: Architectural plans of the studied house. Red points correspond to the data-loggers locations. Z1 to Z8 are the thermal zones as defined in the TRNSYS based computer code.

ANNEX 2

Calculation of the effective thermal conductivity of the air gap in the cavity wall system and the hollow core slab.

FIGURE 2.1. Scheme of the cavity wall.

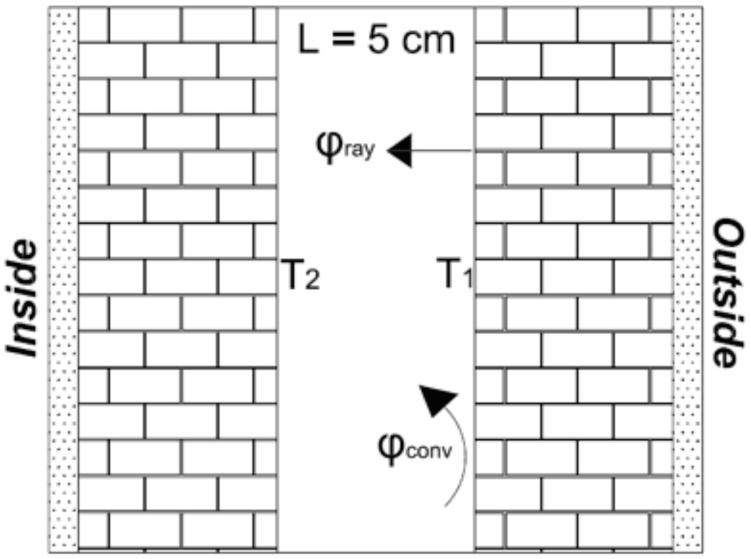

The cavity wall system is constituted by two walls of red brick blocs separated by an air gap with a width of L = 5 cm. The height of the air gap is H = 2.8 m (Fig. 2.1). This air space is subject to heat transfer between the internal surfaces of the walls whose temperatures are T_1 and T_2. The total heat flux between these surfaces is,

$$\varphi_g = \varphi_{conv} + \varphi_{rad} + \varphi_{cond} \tag{2.1}$$

As the thermal conductivity of air is low, conduction heat flux through the air gap φ_{cond} may be neglected. The global heat flux may be written as follows,

$$\varphi_g = \varphi_{conv} + \varphi_{rad} = [\,k_{eff}\,.\,(T_1 - T_2)]/L \tag{2.2}$$

Where k_{eff} is the effective thermal conductivity of the cavity wall air gap assimilated to a pure conductive medium.

Therefore, the effective thermal conductivity of the cavity wall air gap may calculated by the following equation,

$$k_{eff} = [L\,.\,\varphi_g]/(T_1 - T_2) \tag{2.3}$$

A.2.1 Calculation of the convection heat flux

Convection heat flux between the internal surfaces of the cavity wall is,

$$\varphi_{conv} = h_m\,(T_1\text{-}T_2) \tag{2.4}$$

The convection heat transfer coefficient at the internal surfaces the walls is defined by,

$$h_m = (Nu.k_{eff})/L \tag{2.5}$$

Correlations for the Nusselt Number in large aspect ratio inclined enclosures may be found in [34-36]. In the case of a vertical enclosure, the Nusselt number is given by the maximum of the values calculated by the following equations [34, 35]

$$Nu_1 = 0.0605 \cdot Ra_L^{1/3} \tag{2.6}$$

$$Nu_2 = \left\{1 + \left[\frac{0.104 \cdot Ra_L^{0.293}}{1+(6310/Ra_L)^{1.36}}\right]^3\right\}^{1/3} \tag{2.7}$$

$$Nu_3 = 0.242 \left(\frac{Ra_L}{H/L}\right)^{0.272} \tag{2.8}$$

Where Ra_L is the Rayleigh number based on the width of the air gap,

$$Ra_L = [g.\beta.(T_1 - T_2).L^3]/(\upsilon.\alpha) \tag{2.9}$$

Eqs (2.6-8) are valid for $10^3 < RaL < 10^7$ and an aspect ratio H/L > 10. The latter condition is verified in the present case, as H/L = 56.

A.2.2 Calculation of the radiation heat flux:

Radiation flux between the internal surfaces of the cavity wall is given by [24],

$$\varphi_{rad} = \left[\sigma\,(T_1^4 - T_2^4)\right]/\left(\frac{1}{\varepsilon_1} + \frac{1}{\varepsilon_2} - 1\right) \tag{2.10}$$

Where ε is the emissivity of the red clay block walls which is taken to be 0.9 [19].

The walls internal surface temperatures T_1 and T_2 depend on the climate conditions. It is assumed that these temperatures are constants and equal to 45°C and 34°C respectively at the outside (T_1) and inside (T_2) walls inner surfaces. It is believed that this is the worst case leading to the greatest heat flux and thus lowest effective thermal resistance of the cavity wall.

The value of Rayleigh number is then $Ra_L = 1.1\ 10^5$ which is in the range of the validity of Eqs (2.6-8).

Thermal properties of air at 40°C are [24]:

$\upsilon = 16.97$ 10-6 $m^2.s^{-1}$; $\alpha = 23.02\ 10^{-6}\ m^2.s^{-1}$; $k = 0.0271\ W.m^{-1}.K^{-1}$; $\beta = 3.2\ 10^{-3}\ K^{-1}$; $Pr = 0.708$

The resulting heat transfer fluxes are $\varphi_{conv} = 18.5\ W.m^{-2}$ and $\varphi_{rad} = 52.9\ W.m^{-2}$. Thus total heat flux between the internal surfaces of the walls is $\varphi g = 71.4\ W.m^{-2}$ and the effective thermal conductivity of our cavity wall is $k_{eff} = 0.324\ W.m^{-1}.K^{-1}$.

The Hollow Core Slab is constituted by two concrete slabs separated by an air gap of L = 5 cm width. The length of the air space is H = 7.95 m (Fig. 2.2). Its effective thermal conductivity may be calculated from similar correlation than the cavity wall for horizontal enclosures [34, 36],

$$Nu = 1 + 1.44\left[1 - \frac{1708}{Ra_L}\right] + \left[\left(\frac{Ra_L}{5830}\right)^{1/3} - 1\right] \tag{2.11}$$

Eq. (2.11) is valid for $Ra_L \leq 10^8$ and an aspect ratio H/L > 10. The latter is verified in the present case (H/L = 159).

The slabs' surface temperatures, which depend on the climate conditions, are assumed constants and equal to 50°C and 34°C respectively at the outside (T_1) and inside (T_2) slab inner surfaces. Again, it is believed that this is the worst case leading to the lowest effective

thermal resistance of the hollow core slab. The value of Rayleigh number is then $Ra_L = 1.6\ 10^5$ which is in the range of the validity of Eq. (2.11).

The Hollow Core Slab considered in this paper is equipped with a radiant barrier. Thus, radiation heat flux is almost negligible due the low emissivity of the radiant barrier.

The resulting heat transfer flux is $\varphi_{conv} = 38.5\ W.m^{-2}$. Thus the effective thermal conductivity of the Hollow Core Slab air gap is $k_{eff} = 0.12\ W.m^{-1}.K^{-1}$.

FIGURE 2.2. Scheme of the Hollow Core Slab with radiant barrier.

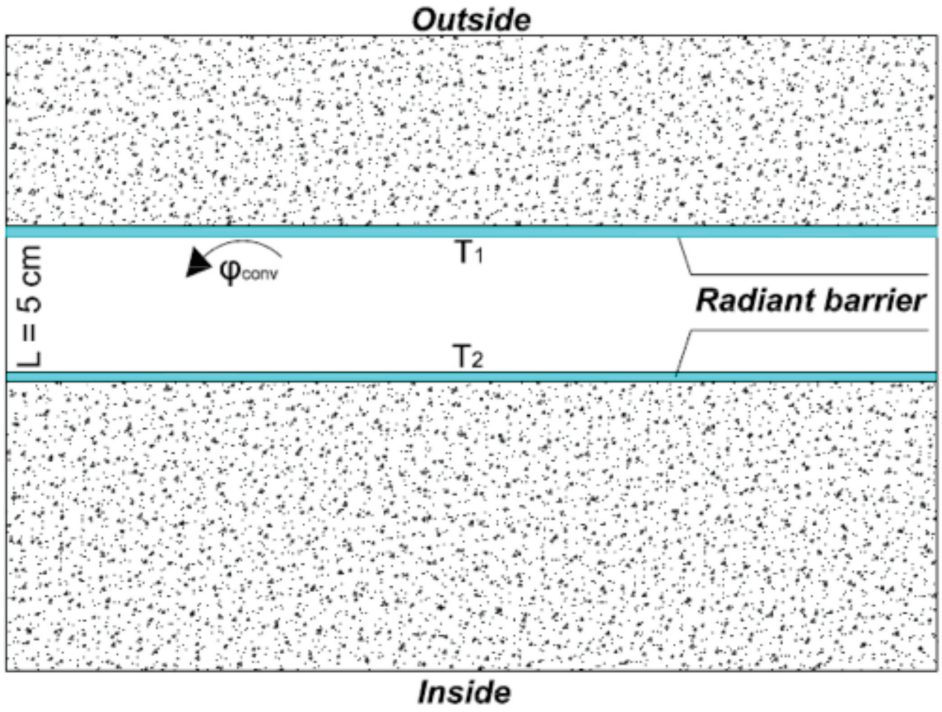

It is important to mention that the above calculated effective thermal conductivities are in accordance with the available results in the literature, if the radiation heat flux is neglected [19]. Indeed, the ASHRAE recommendation for a 5 cm vertical air space (without radiant barrier) suggests an effective thermal conductivity of $0.25\ W.m^{-1}.K^{-1}$ [19], which is 30% higher than the calculated cavity wall effective thermal conductivity as thermal convection was not taken into account in the ASHRAE document.

Regarding the radiant barrier, it significantly lowers thermal radiation heat transfer. However, radiation heat flux is not zero. According to our calculations, this heat flux may be estimated to $5\ W.m^{-2}$, which would raise the effective thermal conductivity of the HCS to around $0.14\ W.m^{-1}.K^{-1}$. The latter results in the heat transmission coefficient to be $1.08\ W.m^{-2}.K^{-1}$. It was checked that neglecting complete radiation heat transfer in the HCS with a radiant barrier, which is the case in this study, results in an error of less than 1% in terms of the house annual thermal load.